Rapid #: -19150588

CROSS REF ID: **872515**

LENDER: **LN1 :: Dixson Library**

BORROWER: **ORU :: Main Library**

TYPE:	Article CC:CCL
JOURNAL TITLE:	Contributions to mineralogy and petrology
USER JOURNAL TITLE:	Contributions to mineralogy and petrology.
ARTICLE TITLE:	Heat Capacity of minerals in the system Na2O-K2O-CaO-MgO-FeO-Fe2O3-Al2O3-SiO2-TiO2-H2O-CO2:representation, estimation, and high temperature extrapolation
ARTICLE AUTHOR:	Berman, R. G., and Brown, T. H.
VOLUME:	89
ISSUE:	
MONTH:	
YEAR:	1966
PAGES:	168-183
ISSN:	0010-7999
OCLC #:	1142566

Processed by RapidX: 6/8/2022 5:38:40 PM

3

Rapid #: -19150588

RapidX Upload

Status	Rapid Code	Branch Name	Start Date
New	ORU	Main Library	06/08/2022 05:25 AM
Pending	LJ0	Main Library	06/08/2022 05:26 AM
Unfilled	LJ0	Main Library	06/08/2022 10:42 AM
Pending	LN1	Dixson Library	06/08/2022 10:43 AM

CALL #: P549.05 CON

LOCATION: LN1 :: Dixson Library :: DIXSON_LIB DIXSON_JNL

REQUEST TYPE:	Article CC:CCL
JOURNAL TITLE:	Contributions to mineralogy and petrology
USER JOURNAL TITLE:	Contributions to mineralogy and petrology.
LN1 CATALOG TITLE:	Contributions to mineralogy and petrology
ARTICLE TITLE:	Heat Capacity of minerals in the system Na2O-K2O-CaO-MgO-FeO-Fe2O3-Al2O3-SiO2-TiO2-H2O-CO2:representation, estimation, and high temperature extrapolation
ARTICLE AUTHOR:	Berman, R. G., and Brown, T. H.
VOLUME:	89
ISSUE:	
MONTH:	
YEAR:	1966
PAGES:	168-183
ISSN:	0010-7999
OCLC #:	1142566 LN1 OCLC #: 1030250
CROSS REFERENCE ID:	[TN:872515][ODYSSEY:184.171.112.14/ORU]
VERIFIED:	

BORROWER: ORU :: Main Library

ExLibris RapidILL

Contrib Mineral Petrol (1985) 89:168–183

Contributions to Mineralogy and Petrology

Heat capacity of minerals in the system $Na_2O-K_2O-CaO-MgO-FeO-Fe_2O_3-Al_2O_3-SiO_2-TiO_2-H_2O-CO_2$: representation, estimation, and high temperature extrapolation

Robert G. Berman and Thomas H. Brown
Department of Geological Sciences, University of British Columbia, Vancouver, B.C., Canada V6T 2B4

Abstract. A revised equation is proposed to represent and extrapolate the heat capacity of minerals as a function of temperature:

$C_P = k_0 + k_1 T^{-0.5} + k_2 T^{-2} + k_3 T^{-3}$ (where $k_1, k_2 \leq 0$).

This equation reproduces calorimetric data within the estimated precision of the measurements, and results in residuals for most minerals that are randomly distributed as a function of temperature. Regression residuals are generally slightly greater than those calculated with the five parameter equation proposed by Haas and Fisher (1976), but are significantly lower than those calculated with the three parameter equation of Maier and Kelley (1932).

The revised equation ensures that heat capacity approaches the high temperature limit predicted by lattice vibrational theory ($C_P = 3R + \alpha^2 VT/\beta$). For 16 minerals for which α and β have been measured, the average C_P at 3,000 K calculated with the theoretically derived equation ranges from 26.8 ± 0.8 to 29.3 ± 1.9 J/(afu·K) (afu = atoms per formula unit), depending on the assumed temperature dependence of α. For 91 minerals for which calorimetric data above 400 K are available, the average C_P at 3,000 K calculated with our equation is 28.3 ± 2.0 J/(afu·K). This agreement suggests that heat capacity extrapolations should be reliable to considerably higher temperatures than those at which calorimetric data are available, so that thermodynamic calculations can be applied with confidence to a variety of high temperature petrologic problems.

Available calorimetric data above 250 K are fit with the revised equation, and derived coefficients are presented for 99 minerals of geologic interest. The heat capacity of other minerals can be estimated (generally within 2%) by summation of tabulated 'oxide component' C_P coefficients which were obtained by least squares regression of this data base.

Introduction

Knowledge of the heat capacity of minerals is fundamental to the description of their thermodynamic behavior. While heat capacity can be determined by a variety of calorimetric techniques, adequate representation of these data as a function of temperature is necessary to provide for interpolation between the temperatures of the calorimetric measurements. This interpolation facilitates accurate thermodynamic calculations applicable to a variety of petrologic problems, one important example being the evaluation of the thermodynamic properties of minerals on the basis of phase equilibrium experiments (Helgeson et al. 1978; Robinson et al. 1982; Berman et al. 1984).

Ever since Maier and Kelley (1932) proposed an empirical equation for the representation of the temperature dependence of the heat capacity of minerals, the use of such equations, formulated as power series in temperature, has become common practice. As summarized in Table 1, the Maier-Kelley equation contains only three terms, whereas the equation proposed by Haas and Fisher (1976) uses two additional parameters in order to reproduce the calorimetric measurements more precisely.

As stressed repeatedly (e.g. Robie et al. 1979; Haas et al. 1981; Robinson and Haas 1983), the Haas-Fisher and Maier-Kelley equations are suited to represent the variation of heat capacity with temperature only *within* the temperature range of the data. Because calorimetric data for many phases are available only at temperatures lower than are needed for many petrologic applications, it is desirable to have a function which allows for reliable extrapolation beyond the highest temperature of calorimetric measurement.

Lane and Ganguly (1980) and Holland (1981) proposed that extrapolations of heat capacity (using the HF equation without the 'fT^2' term) for a given mineral be controlled by estimating high temperature heat capacity from reactions (assuming that $\Delta C_P = 0$) involving other minerals for which data have been measured at higher temperatures. The drawback of this approach is that it is path-dependent, and there is no a priori method for selecting one possible reaction over another. In addition, errors in the heat capacity of any of the minerals in the selected reaction become

Table 1: Heat Capacity Equations

Source of Equations	Terms in C_P Equations						
	T^2	T^1	T^0	$T^{-0.5}$	T^{-1}	T^{-2}	T^{-3}
Maier and Kelley (1932)		b	a			c	
Haas and Fisher (1976)	f	b	a	g		c	
Berman and Brown (1983)			a	$g \leq 0$	$h \leq 0$	$c \leq 0$	
Berman and Brown (this paper)			k_0	$k_1 \leq 0$		$k_2 \leq 0$	k_3

Offprint requests to: R.G. Berman

incorporated in the estimated heat capacity data points. In this paper we propose a revised heat capacity equation that provides a general technique for the extrapolation of the heat capactiy of minerals to high temperature.

High temperature C_P extrapolation

Theoretical constraints

The heat capacity of solids arises from vibration of atoms in a three dimensional lattice. Einstein (1907) and Debye (1912) derived equations for the temperature dependence of C_V, the heat capacity at constant volume, based on the assumption that atoms behave as harmonic oscillators at points within a crystal lattice. Although only the Debye equation leads to the 'T^3' relationship observed at low temperatures for non-conducting solids, both equations predict that C_V approaches $3R$/afu (R is the gas constant, afu = atoms/formula unit) at high temperatures. This so-called "limit of Petit and Dulong" (1819), which was initially based on their measurements of the heat capacity of solid elements, can also be derived from classical kinetic theory (Boltzmann 1871).

The heat capacity at constant pressure, C_P, is related to C_V by

$$C_P = C_V + \alpha^2 VT/\beta \tag{1}$$

where α is the coefficient of thermal expansion, β is the coefficient of compressibility, T is the absolute temperature, and V is the volume. Thus, at high temperature, C_P approaches the limit given by

$$C_P = 3R + (\alpha^2 V/\beta)T \tag{2}$$

Although anharmonicity and electronic contributions can lead to small departures from the $3R$ limit, the main difficulty in use of equation 2 stems from uncertainties in the variation of α and β with temperature. The limited data available (e.g. the data of Raz (1983) for quartz, and of Sumino et al. (1983) for periclase) suggest however that α and β vary sympathetically, and that the quantity α/β can be considered constant above the Debye temperature. Precise thermal expansion data for the aluminosilicates (Winter and Ghose 1979) indicate that the values of $(\partial V/\partial T)$ are constant up to 1,600 K, which implies that thermal expansivities ($\alpha = 1/V(\partial V/\partial T)_p$) may decrease with increasing temperature. Alternately, high temperature volumetric data for most minerals can be accurately fit by

$$V = V_{298}\, e^{[a(T-T_r) + b/2(T^2 - T_r^2)]} \tag{3}$$

which results from the assumption that

$$\alpha = a + bT \tag{4}$$

Substitution of equation 4 into equation 2 yields

$$C_p = 3R + (\alpha/\beta Va)\,T + (\alpha/\beta Vb)\,T^2 \tag{5}$$

For 16 minerals for which high temperature and pressure volumetric measurements are available, heat capacity has been calculated at 3,000 K (arbitrarily chosen as an upper temperature limit for most geologic applications) with equations 2 (assuming constant α's, evaluated at the highest temperatures at which data are available) and 5. On an atomic basis, the results are quite uniform (Table 2, columns 1 and 2), with the average heat capacity at 3,000 K for these minerals between 26.8 ± 0.8 and 29.3 ± 1.9 J/(afu·K). The differences between the two sets of values indicate that uncertainties in the temperature dependence of α and β lead to uncertainties of approximately 10% in high temperature heat capacity.

Table 2. Comparison between heat capacity at 3,000 K in J/(afu·K)[a] predicted theoretically and extrapolated with empirical equations

Mineral	Predicted[b]		Extrapolated[c]		
	Eq. 2	Eq. 5	BB	MK	HF
Albite	25.87	27.38	26.98	33.19	42.54
Almandine	27.07	30.61	27.19	31.46	16.93
Andalusite	26.55	28.92	27.15	34.71	48.55
Anorthite	25.27	25.32	28.55	35.79	52.11
Calcite	26.33	31.09	31.20	49.91	98.58
Corundum	27.69	29.84	27.90	30.83	32.00
Diopside	26.53	28.53	27.53	35.12	47.45
Enstatite	26.62	28.37	26.08	30.47	39.09
Fayalite	27.02	28.49	30.54	36.35	59.41
Forsterite	28.52	33.60	28.87	33.77	25.79
Grossularite	26.71	29.15	25.76	38.23	72.32
Jadeite	27.28	31.49	27.41	36.48	44.52
Kyanite	26.34	28.02	27.56	36.22	51.75
Lime	27.34	29.84	28.11	31.82	60.60
Periclase	27.46	30.09	27.82	30.86	29.09
Sillimanite	25.93	28.38	26.77	35.55	67.13

[a] afu = atom/formula unit.
[b] Predicted heat capacities at 3,000 K using equations 2 and 5, with α's and β's given by Skinner (1966) and Birch (1966), respectively.
[c] Extrapolated heat capacities at 3,000 K resulting from regression analysis of calorimetric data for each phase with the Maier-Kelley equation (MK), the Haas-Fisher (HF), and with equation 7 (BB). Data below 300 K were not included in regression analysis with the MK equation.

Calculations with Empirical Equations

Extrapolations with the Haas-Fisher (HF) and Maier-Kelley (MK) equations are not in accord with these calculations, but it should be remembered that these equations were not developed as extrapolative tools, and potential users of the HF equation have been repeatedly cautioned against such use of this equation. We reemphasize this warning by tabulating high temperature C_P values for several minerals calculated with both the MK and HF equations. Without additional constraints such as discussed by Lane and Ganguly (1980) and Holland (1981), the HF equation is not suited to the purpose of extrapolation (Table 2, column 5) because the use of five terms, unconstrained in sign, often produces inflections or maxima in the C_P versus T curve outside the range of the data. The MK equation leads to unreasonably high values for heat capacities at elevated temperatures (Table 2, column 4) because of the increasing contribution at high temperatures of the 'bT' term, although, for some phases with anomalously low high temperature heat capacity (e.g. quartz, pyrope), the MK extrapolations may appear to be in accord with the average theoretically derived high temperature heat capacities.

Heat capacity calculated from empirical equations can be constrained to approach a high temperature limit by

using an equation of the form

$$C_P = k_0 + \sum_i k_i T^{-i/2}. \quad (6)$$

Because heat capacity will approach the value given by k_0 at high temperatures, this equation is most suitable for representation of C_V. Equations 2 and 5 indicate that empirical equations for heat capacity should include T and possibly T^2 terms, but practical considerations justify exclusion of these terms. Our analysis of calorimetric data with equations including either T or T^2 terms generally results in high temperature heat capacity considerably higher than the values calculated with either equations 2 or 5, because these terms, which increasingly contribute to C_P at high temperatures, are poorly constrained by calorimetric data which commonly have not been obtained above 1,000 K. In principle, the coefficients of these terms could be evaluated from volumetric data (using eqs. 2 or 5), but accurate data are presently available for too few minerals for this method to be of general utility. Moreover, regression analysis of data with selected terms of equation 6 results in $(\partial C_P/\partial T)$ values that are positive even at temperatures as high as 3,000 K. In practive, then, calculations with equation 6 yield reasonable approximations of the temperature dependence of heat capacity, and, as discussed in the next section, result in excellent agreement with the theoretical values derived above.

In previous work (Berman and Brown 1983; 1984), it has been found that use of the T^0, $T^{-0.5}$, T^{-1}, and T^{-2} terms of equation 6 adequately reproduces heat capacity data above 298.15 K, and also results in reasonable high temperature extrapolations. Data below 298.15 K from adiabatic calorimetry cannot be well represented with these terms, however, and, although we are interested primarily in heat capacity above 298.15 K, the more accurate adiabatic calorimetric data provide important constraints on heat capacity just above 298.15 K. Robie et al. (1979), for instance, use $(\partial C_P/\partial T)$ derived from adiabatic calorimetry measurements to constrain their fit of high temperature data. In order to fit the low temperature data adequately, we have found it necessary to use a term which allows for a positive contribution to the C_P at low temperatures. We have selected the '$k_3 T^{-3}$' term because its contribution to C_P rapidly decreases at high temperatures, and it preserves the reliability of high temperature extrapolations, even if k_3 is positive. Our revised heat capacity equation is:

$$C_P = k_0 + k_1 T^{-0.5} + k_2 T^{-2} + k_3 T^{-3} (k_1, k_2 \leq 0) \quad (7)$$

C_P versus T curves calculated with equation 7 contain no inflections or maxima at high temperatures because the parameters which dominate at high temperatures are powers of $(1/T)$ and k_1 and k_2 are constrained to be negative. Equation 7 can not be used below the lowest temperature data (in this paper we fit data above approximately 250 K), because calculated heat capacities may contain minima at low temperatures if k_3 is positive.

The form of equation 7 makes it unsuitable for the representation of the rapid increase in heat capacity observed for phases which undergo lambda transitions. For a phase with a lambda transition at T_λ, heat capacity can be computed from

$$C_P = k_0 + k_1 T^{-0.5} + k_2 T^{-2} + k_3 T^{-3} + C_{P_\lambda} \quad (8)$$

where, for $T_{ref} \leq T \leq T_\lambda$, C_{P_λ} is given by

$$C_{P_\lambda} = T(l_1 + l_2 T)^2 \quad (9)$$

For $T > T_\lambda$, heat capacity is calculated using the first four terms of equation 8, equivalent to equation 7. Equations 8 and 9 represent measured calorimetric data adequately, with the exception of data at temperatures within the immediate vicinity (usually 10–30°) of the transition. A major advantage of using these equations to represent the heat capacity of phases which undergo lambda transitions, is that the thermodynamic properties of these phases can be calculated at elevated pressures if $(\partial P/\partial T)$ of the transition is known or can be estimated (see Appendix 2).

Evaluation of heat capacity data

Heat capacity coefficients of equation 8 have been determined for minerals in the system $Na_2O-K_2O-CaO-MgO-FeO-Fe_2O_3-Al_2O_3-SiO_2-TiO_2-H_2O-CO_2$ by weighted linear regression of available calorimetric data. Details of the analytical procedure are described in Appendix 1. Resulting C_P coefficients are given in Table 3, along with the temperature range of the data used in the analysis and the average absolute deviations of the derived functions from each set of data.

Table 3: Coefficients for calculation of heat capacity (J/mol·K) with equation 8

Mineral	Formula	k_0	$k_1 \times 10^{-2}$	$k_2 \times 10^{-5}$	$k_3 \times 10^{-7}$	Range(K)	AAD[a]	Reference
Acmite	$NaFeSi_2O_6$	352.46	−30.904	−0.792	−6.427	249– 307	0.17	Ko et al. (1977)
						402–1103	0.13	Ko et al. (1977)
Akermanite	$Ca_2MgSi_2O_7$	389.64	−29.656	0.0	−18.333	256– 296	0.21	Weller and Kelley (1963)
						432–1605	0.26	Pankratz and Kelley (1964b)
Albite (high)	$NaAlSi_3O_8$	391.87	−22.696	−93.975	132.604	250– 380	0.04	Haselton et al. (1983)
						339– 997	0.35	Hemingway et al. (1981)
						1360–1361	0.50	Stebbins et al. (1983)
Albite (low)	$NaAlSi_3O_8$	393.64	−24.155	−78.928	107.064	250– 370	0.11	Openshaw et al. (1976)
						339– 997	0.65	Hemingway et al. (1981)
						472–1270	0.47	Kelley et al. (1953)
						373–1373	0.27	White (1919)
Analcime	$NaAlSi_2O_6 \cdot H_2O$	571.83	−71.887	0.0	149.306	290– 347	0.45	Johnson et al. (1982)
						349– 623	0.21	Johnson et al. (1982)

Table 3 (continued)

Mineral	Formula	k_0	$k_1 \times 10^{-2}$	$k_2 \times 10^{-5}$	$k_3 \times 10^{-7}$	Range(K)	AAD[a]	Reference
Anatase	TiO_2	78.10	0.0	−31.251	32.912	256–295	0.04	Shomate (1947)
						545–1304	0.26	Naylor (1946)
Andalusite	Al_2SiO_5	241.88	−13.146	−61.355	70.692	254–377	0.13	Robie and Hemingway (1984)
						397–1601	0.16	Pankratz and Kelley (1964a)
Anorthite	$CaAl_2Si_2O_8$	439.37	−37.341	0.0	−31.702	292–381	0.08	Robie et al. (1978)
						349–986	0.40	Krupka et al. (1979)
						373–1673	0.30	White (1919)
Anthophyllite	$Mg_7Si_8O_{22}(OH)_2$	1219.31	−57.665	−347.661	440.090	250–385	0.07	Krupka et al. (1985a)
						344–679	0.46	Krupka et al. (1985b)
Antigorite[e]	$Mg_{48}Si_{34}O_{85}(OH)_{62}$	9011.99	−630.981	−1459.624	1907.022	256–296	0.06	King et al. (1967)
						405–847	0.12	King et al. (1967)
Aragonite	$CaCO_3$	166.62	−14.994	0.0	5.449	252–291	0.40	Staveley and Linford (1969)
						299–572	0.37	Kobayashi (1951)
Boehmite	AlO(OH)	152.49	−14.433	0.0	−9.320	256–296	0.08	Shomate and Cook (1946)
Bronzite	$Fe_{0.15}Mg_{0.85}Si_3O_3$	161.45	−10.546	−29.323	37.992	250–387	0.06	Krupka et al. (1985a)
						345–1000	0.35	Krupka et al. (1985b)
Brucite	$Mg(OH)_2$	136.84	−5.371	−43.619	55.269	253–299	0.32	Giauque and Archibald (1937)
						350–666	0.16	King et al. (1975)
Ca–Al pyroxene	$CaAl_2SiO_6$	310.70	−16.716	−74.553	94.878	253–379	0.13	Haselton et al. (1984)
						350–859	0.40	Perkins (unpublished data)
Calcite	$CaCO_3$	193.24	−20.409	0.0	19.946	257–286	0.35	Staveley and Linford (1969)
						345–780	0.48	Jacobs et al. (1981)
Calcium aluminate	$CaAl_2O_4$	227.04	−16.691	−5.608	−8.554	256–296	0.16	King (1955a)
						402–1800	0.33	Bonnickson (1955a)
Calcium dialuminate	$CaAl_4O_7$	337.98	−10.222	−121.126	151.060	256–296	0.10	King (1955a)
						403–1801	0.27	Bonnickson (1955a)
Calcium ferrite	$CaFe_2O_4$	208.52	−8.471	0.0	−15.559	256–296	0.07	King (1954)
						549–1229	0.16	Bonnickson (1954)
Carnieigite	$NaAlSiO_4$	232.69	−15.158	−57.552	99.999	389–1697	0.24	Kelley et al. (1953)
$\alpha=\beta$[b]		970	8741	−11.472	34.895			
Chrysotile[e]	$Mg_3Si_2O_5(OH)_4$	539.77	−30.723	−144.626	197.376	256–296	0.03	King et al. (1967)
Cordierite	$Mg_2Al_4Si_5O_{18}$	937.62	−71.663	−110.231	142.574	256–296	0.07	Weller and Kelley (1963)
						400–1652	0.13	Pankratz and Kelley (1964b)
Corundum	Al_2O_3	155.02	−8.284	−38.614	40.908	250–290	0.03	Ditmars and Douglas (1971)
						300–2300	0.11	Ditmars and Douglas (1971)
Cristobalite	SiO_2	83.51	−3.747	−24.554	28.007	272–297	0.72	Anderson (1936)
$\alpha=\beta$[b]		535	1073	−29.079	90.291	360–524	1.21	Thompson and Wennemer (1979)
						373–1673	0.07	White (1919)
						1007–1834	0.12	Richet et al. (1982)
Dehydrated analcime	$NaAlSi_2O_6$	401.27	−42.480	0.0	21.630	257–347	0.16	Johnson et al. (1982)
						407–702	0.08	Pankratz (1968)
Dehydrated muscovite[d]	$KAl_3Si_3O_{11}$	585.19	−42.741	−64.146	57.965	401–1203	0.12	Pankratz (1964)
Diaspore	AlO(OH)	143.24	−15.404	−3.231	6.463	256–295	0.07	King and Weller (1961a)
						340–509	0.18	Perkins et al. (1979)
Dicalcium ferrite	$Ca_2Fe_2O_5$	253.12	0.0	−84.588	91.229	255–296	0.13	King (1954)
						376–1703	0.55	Bonnickson (1954)
Dickite[e]	$Al_2Si_2O_5(OH)_4$	525.18	−36.434	−130.862	192.739	256–296	0.06	King and Weller (1961a)
Diopside	$CaMgSi_2O_6$	305.41	−16.049	−71.660	92.184	256–295	0.18	King (1957)
						254–381	0.09	Krupka et al. (1985a)
						344–999	0.53	Krupka et al. (1985b)
						373–1523	0.12	White (1919)
						573–1573	0.43	Wagner (1932)

Table 3 (continued)

Mineral	Formula	k_0	$k_1 \times 10^{-2}$	$k_2 \times 10^{-5}$	$k_3 \times 10^{-7}$	Range(K)	AAD[a]	Reference
Dolomite	$CaMg(CO_3)_2$	368.02	−37.508	0.0	18.079	250– 300	0.04	Stout and Robie (1963)
						349– 650	0.35	Krupka et al. (1985b)
Enstatite (clino)	$MgSiO_3$	139.96	−4.970	−44.002	53.571	256– 295	0.20	Kelley (1943)
						373– 773	0.73	White (1919)
						573–1573	0.77	Wagner (1932)
Enstatite (ortho)	$MgSiO_3$	166.99	−12.043	−23.378	29.398	254– 385	0.05	Krupka et al. (1985a)
						344– 999	0.37	Krupka et al. (1985b)
						973–1273	0.98	Haselton (1979)
Epidote[d]	$Ca_2FeAl_2Si_3O_{12}(OH)$	643.85	−30.870	−140.917	154.457	335–1100	0.35	Kiseleva et al. (1974)
Fayalite	Fe_2SiO_4	248.93	−19.239	0.0	−13.910	255– 362	0.19	Robie et al. (1982a)
						492–1370	0.19	Orr (1953)
Forsterite	Mg_2SiO_4	238.64	−20.013	0.0	−11.624	253– 299	0.08	Robie et al. (1982b)
						304– 380	0.89	Robie et al. (1982b)
						398–1807	0.20	Orr (1953)
Gehlenite	$Ca_2Al_2SiO_7$	373.09	−22.768	−47.785	47.791	276– 296	0.07	Weller and Kelley (1963)
						402–1801	0.10	Pankratz and Kelley (1964b)
Geikelite	$MgTiO_3$	146.20	−4.160	−39.998	40.233	256– 296	0.26	Shomate (1946)
						402–1719	0.73	Naylor and Cook (1946)
Gibbsite	$Al(OH)_3$	282.48	−33.999	0.0	16.235	254– 379	0.05	Hemingway et al. (1977)
						339– 479	0.87	Hemingway et al. (1977)
Grossularite	$Ca_3Al_2Si_3O_{12}$	519.40	−0.631	−280.063	351.073	255– 296	0.14	Kolesnik et al. (1979)
						250– 343	0.36	Haselton and Westrum (1980)
						350– 987	0.96	Krupka et al. (1979)
						973–1273	0.89	Haselton (1979)
Halloysite[c]	$Al_2Si_2O_5(OH)_4$	551.52	−47.251	−53.521	74.696	256– 295	0.03	King and Weller (1961a)
Hematite	Fe_2O_3	146.86	0.0	−55.768	52.563	258– 345	0.30	Gronvold and Westrum (1959)
$\alpha=\beta$[b]		955	1287	−15.143	57.116	301– 940	0.66	Gronvold and Samuelsen (1975)
						374–1757	0.36	Coughlin et al. (1951)
Ilmenite	$FeTiO_3$	164.47	−9.905	−5.092	−4.875	256– 296	0.04	Shomate (1946)
						375–1237	0.29	Naylor and Cook (1946)
Jadeite	$NaAlSi_2O_6$	311.29	−20.051	−53.503	66.257	266– 296	0.07	Kelley et al. (1953)
						393–1189	0.12	Kelley et al. (1953)
Kaliophyllite	$KAlSiO_4$	186.00	0.0	−131.067	213.893	287– 296	0.14	Kelley et al. (1953)
$\alpha=\beta$[b]		810	1154	−14.516	44.350	409–1799	0.27	Pankratz (1968)
Kaolinite	$Al_2Si_2O_5(OH)_4$	523.23	−44.267	−22.443	9.231	256– 296	0.11	King and Weller (1961a)
						340– 560	0.43	Hemingway et al. (1978)
Kyanite	Al_2SiO_5	246.63	−13.940	−64.082	75.224	252– 370	0.09	Robie and Hemingway (1984)
						390–1503	0.15	Pankratz and Kelley (1964a)
Larnite (γ)	Ca_2SiO_4	255.22	−23.408	0.0	14.104	256– 286	0.56	King (1957)
						602–1112	0.14	Coughlin and O'Brien (1957)
Larnite	Ca_2SiO_4	209.68	−7.019	−79.894	129.748	266– 296	0.46	Todd (1951)
$\beta=\alpha'$[b]		970	1748	0.0	0.0	406–1816	0.31	Coughlin and O'Brien (1957)
$\alpha'=\alpha$[b]		1710	11903	−46.668	47.447			
Lawsonite	$CaAl_2Si_2O_7(OH)_2 \cdot H_2O$	728.67	−82.481	0.0	85.056	259– 320	0.38	Perkins et al. (1980)
						319– 600	0.30	Perkins et al. (1980)
Leonhardite[c]	$Ca_2Al_4Si_8O_{24} \cdot 7H_2O$	1650.82	−84.120	−234.689	137.222	256– 296	0.13	King and Weller (1961b)
Leucite	$KAlSi_2O_6$	271.14	−9.441	−78.572	95.920	256– 296	0.10	Kelley et al. (1953)
$\alpha=\beta$[b]		955	256	−19.904	68.994	409–1798	0.12	Pankratz (1968)
Lime	CaO	58.79	−1.339	−11.471	10.298	250– 300	0.10	Gmelin (1969)
						563–1176	0.73	Lander (1951)
Magnesite	$MgCO_3$	194.08	−21.210	−1.533	17.491	288– 383	0.03	Hemingway et al. (1977)
						500– 750	0.04	Kelley (1960)
Magnesium ferrite	$MgFe_2O_4$	196.66	0.0	−74.922	81.007	256– 296	0.32	King (1954)
						362–1827	0.38	Bonnickson (1954)
$\alpha=\beta$[b]		665	931	31.165	−109.579			
$\beta=\gamma$[b]		1230	836	0.0	0.0			

Table 3 (continued)

Mineral	Formula	k_0	$k_1 \times 10^{-2}$	$k_2 \times 10^{-5}$	$k_3 \times 10^{-7}$	Range(K)	AAD[a]	Reference
Magnesium titanate[c]	Mg_2TiO_4	226.11	−13.801	−17.011	4.128	256– 296	0.04	Todd (1952)
Magnesium dititanate[c]	$MgTi_2O_5$	232.58	−7.555	−56.608	58.214	256– 296	0.02	Todd (1952)
Magnetite	Fe_3O_4	207.93	0.0	−72.433	66.436	257– 347	0.53	Westrum and Gronvold (1969)
$\alpha=\beta$[b]		848	1565	−39.892	124.851	329– 829	1.09	Gronvold and Sveen (1974)
						351–1825	0.40	Coughlin et al. (1951)
Margarite	$CaAl_4Si_2O_{10}(OH)_2$	680.53	−49.194	−101.611	121.960	255– 345	0.05	Perkins et al. (1980)
						319– 996	0.53	Perkins et al. (1980)
Merwinite	$Ca_3MgSi_2O_8$	453.62	−32.500	0.0	−34.423	286– 296	0.05	Weller and Kelley (1963)
						397–1601	0.13	Pankratz and Kelley (1964b)
Microcline	$KAlSi_3O_8$	381.37	−19.410	−120.373	183.643	250– 370	0.11	Openshaw et al. (1976)
						339– 997	0.60	Hemingway et al. (1981)
Mullite	$Al_6Si_2O_{13}$	634.81	−33.735	−172.099	212.274	256– 296	0.07	Pankratz et al. (1963)
						398–1799	0.30	Pankratz et al. (1963)
Muscovite	$KAl_3Si_3O_{10}(OH)_2$	651.49	−38.732	−185.232	274.247	257– 377	0.15	Robie et al. (1976)
						362– 967	0.40	Krupka et al. (1979)
Natrolite	$Na_2Al_2Si_3O_{10}\cdot 2H_2O$	933.23	−104.790	0.0	87.898	295– 346	0.06	Johnson et al. (1983)
						373– 673	0.17	Johnson et al. (1983)
Nepheline	$NaAlSiO_4$	205.24	−7.599	−108.383	208.182	286– 296	0.56	Kelley et al. (1953)
$\alpha=\beta$[b]		467	241	−102.784	339.448	387–1509	0.41	Kelley et al. (1953)
$\beta=\gamma$[b]		1180	2393	0.0	0.0			
Paragonite[d]	$NaAl_3Si_3O_{10}(OH)_2$	691.91	−53.332	−110.225	162.829	337– 719	0.42	Holland (1979; unpublished data)
Periclase	MgO	61.11	−2.962	−6.212	0.584	250– 269	0.10	Barron et al. (1959)
						250– 320	0.16	Gmelin (1969)
						350– 679	0.41	Krupka et al. (1979)
						373–1173	0.15	Victor and Douglas (1963)
						402–1798	0.25	Pankratz and Kelley (1963)
Perovskite	$CaTiO_3$	150.49	−6.213	0.0	−43.010	286– 296	0.42	Shomate (1946)
						484–1793	0.33	Naylor and Cook (1946)
Portlandite	$Ca(OH)_2$	140.98	−7.986	0.0	−17.852	253– 329	0.36	Hatton et al. (1959)
						314– 670	0.55	Kobayashi (1950)
Potassium silicate[d]	K_2SiO_3	225.99	−19.866	0.0	14.896	403–1103	0.25	Beyer et al. (1980)
Potassium disilicate	$K_2Si_2O_5$	240.72	0.0	−147.934	228.921	283– 308	0.09	Beyer et al. (1980)
						402–1258	0.23	Beyer et al. (1980)
$\alpha=\beta$[b]		510	933	0.0	0.0			
$\beta=\gamma$[b]		867	2744	0.0	0.0			
Prehnite	$Ca_2Al_2Si_3O_{10}(OH)_2$	652.39	−42.318	−121.193	160.044	260– 347	0.03	Perkins et al. (1980)
						319– 790	0.18	Perkins et al. (1980)
Pseudobrookite	Fe_2TiO_5	261.35	−15.307	0.0	−23.466	256– 296	0.09	Todd and King (1953)
						410–1739	0.25	Bonnickson (1955b)
Pseudowollastonite	$CaSiO_3$	153.43	−8.876	−23.567	29.715	275– 295	0.65	Wagner (1932)
						576–1558	0.46	Wagner (1932)
						373–1673	0.22	White (1919)
Pyrope	$Mg_3Al_2Si_3O_{12}$	535.55	−12.414	−196.256	217.002	297– 345	0.11	Haselton and Westrum (1980)
						350–1000	0.31	Newton et al. (1979)
						973–1273	1.05	Haselton (1979)
Pyrophyllite	$Al_2Si_4O_{10}(OH)_2$	665.93	−58.974	−49.799	66.181	254– 304	0.02	Robie et al. (1976)
						332– 679	0.37	Krupka et al. (1979)
Quartz	SiO_2	80.01	−2.403	−35.467	49.157	250– 290	0.19	Westrum (unpublished data)
$\alpha=\beta$[b]		848	499	−18.792	50.334	400– 820	0.32	Ghiorso et al. (1979)
						373–1373	0.19	White (1919)
						1001–1676	0.09	Richet et al. (1982)
Rankinite[c]	$Ca_3Si_2O_7$	339.91	−9.851	−106.610	137.359	256– 296	0.05	King (1957)

Table 3 (continued)

Mineral	Formula	k_0	$k_1 \times 10^{-2}$	$k_2 \times 10^{-5}$	$k_3 \times 10^{-7}$	Range(K)	AAD[a]	Reference
Rutile	TiO_2	77.84	0.0	−33.678	40.294	251– 297	0.10	Shomate (1947)
						762–1746	0.39	Naylor (1946)
Sanidine	$KAlSi_3O_8$	395.49	−24.159	−85.454	121.491	250– 380	0.02	Haselton et al. (1983)
						339– 997	0.53	Hemingway et al. (1981)
Scolecite	$CaAl_2Si_3O_{10} \cdot 3H_2O$	1112.59	−132.421	0.0	97.348	256– 346	0.07	Johnson et al. (1983)
						373– 474	0.37	Johnson et al. (1983)
Siderite	$FeCO_3$	177.36	−16.694	−3.551	15.075	240– 296	0.26	Anderson (1934)
						251– 373	0.24	Robie et al. (1984)
						339– 449	0.36	Robie et al. (1984)
Sillimanite	Al_2SiO_5	235.43	−11.219	−74.363	95.747	253– 378	0.09	Robie and Hemingway (1984)
						401–1496	0.41	Pankratz and Kelley (1964a)
Sodium silicate	Na_2SiO_3	234.77	−22.189	0.0	13.530	259– 294	0.33	Kelley (1939)
						923–1216	0.13	Richet et al. (1984)
Sodium disilicate	$Na_2Si_2O_5$	250.69	0.0	−156.510	221.700	255– 294	0.35	Kelley (1939)
						376– 974	0.95	Naylor (1945a)
Sodium titanate[d]	Na_2TiO_3	198.91	−6.443	−59.486	85.050	388–1096	0.87	Naylor (1945b)
Sodium dititanate[d]	$Na_2Ti_2O_5$	272.57	−12.827	0.0	−15.763	362–1039	0.36	Naylor (1945b)
Sodium trititanate[d]	$Na_2Ti_3O_7$	367.20	−19.403	0.0	−13.706	374–1198	0.31	Naylor (1945b)
Sphene	$CaTiSiO_5$	234.62	−10.403	−51.183	59.146	255– 296	0.08	King et al. (1954)
						375–1495	0.23	King et al. (1954)
Spinel	$MgAl_2O_4$	235.90	−17.666	−17.104	4.062	256– 296	0.13	King (1955a)
						421–1805	0.34	Bonnickson (1955a)
Talc	$Mg_3Si_4O_{10}(OH)_2$	664.11	−51.872	−21.472	−32.737	250– 290	0.62	Robie and Stout (1963)
						349– 639	0.23	Krupka et al. (1985b)
Titanium aluminate	$TiAl_2O_5$	249.29	−13.501	−48.061	51.603	256– 296	0.06	King (1955b)
						411–1803	0.23	Bonnickson (1955b)
Titanomagnetite	Fe_2TiO_4	249.63	−18.174	0.0	−5.453	255– 296	0.10	Todd and King (1953)
						423–1041	0.53	Bonnickson (1955b)
Tremolite	$Ca_2Mg_5Si_8O_{22}(OH)_2$	1141.97	−37.937	−420.313	548.553	250– 300	0.12	Robie and Stout (1963)
						350– 680	0.45	Krupka et al. (1985b)
Tricalcium aluminate	$Ca_3Al_2O_6$	321.58	−12.554	−57.813	66.122	256– 296	0.29	King (1955a)
						373–1807	0.54	Bonnickson (1955a)
Tricalcium silicate	Ca_3SiO_5	321.19	−24.502	−9.948	9.753	256– 296	0.10	Todd (1951)
						573–1773	0.22	Elsner von Gronow and Schwiete (1933)
Wollastonite	$CaSiO_3$	149.07	−6.903	−36.593	48.435	251– 386	0.13	Krupka et al. (1985a)
						344– 999	0.50	Krupka et al. (1985b)
						566–1383	0.48	Wagner (1932)
						573–1373	0.52	Elsner von Gronow and Schwiete (1933)
						484–1423	0.26	Southard (1941)
						973–1433	0.21	White (1919)
Wustite	$Fe_{0.947}O$	65.18	−2.803	0.0	−1.737	276– 296	0.20	Todd and Bonnickson (1951)
						339–1555	0.61	Coughlin et al. (1951)
Zoisite	$Ca_2Al_3Si_3O_{12}(OH)$	751.37	−65.857	−19.308	5.143	257– 317	0.08	Perkins et al. (1980)
						344– 729	0.25	Perkins et al. (1980)

[a] Average absolute percent deviation of data from adopted function
[b] Tabulated values: transition temperature (K), heat of transition (J/mol), l_1 ($\times 10^2$) and l_2 ($\times 10^5$) of equation 9 (see Appendix 2), $T_{ref} = 298.15$ K for all phases except α quartz ($T_{ref} = 373$ K) and α′ larnite ($T_{ref} = 970$ K)
[c] Fit of low temperature data and estimated heat capacity (eqn. 11) between 400 and 1,600 K
[d] Fit of high temperature data and estimated heat capacity (eqn. 11) at 250 and 300 K
[e] Heat content data corrected for antigorite formula used by King et al. (1967)

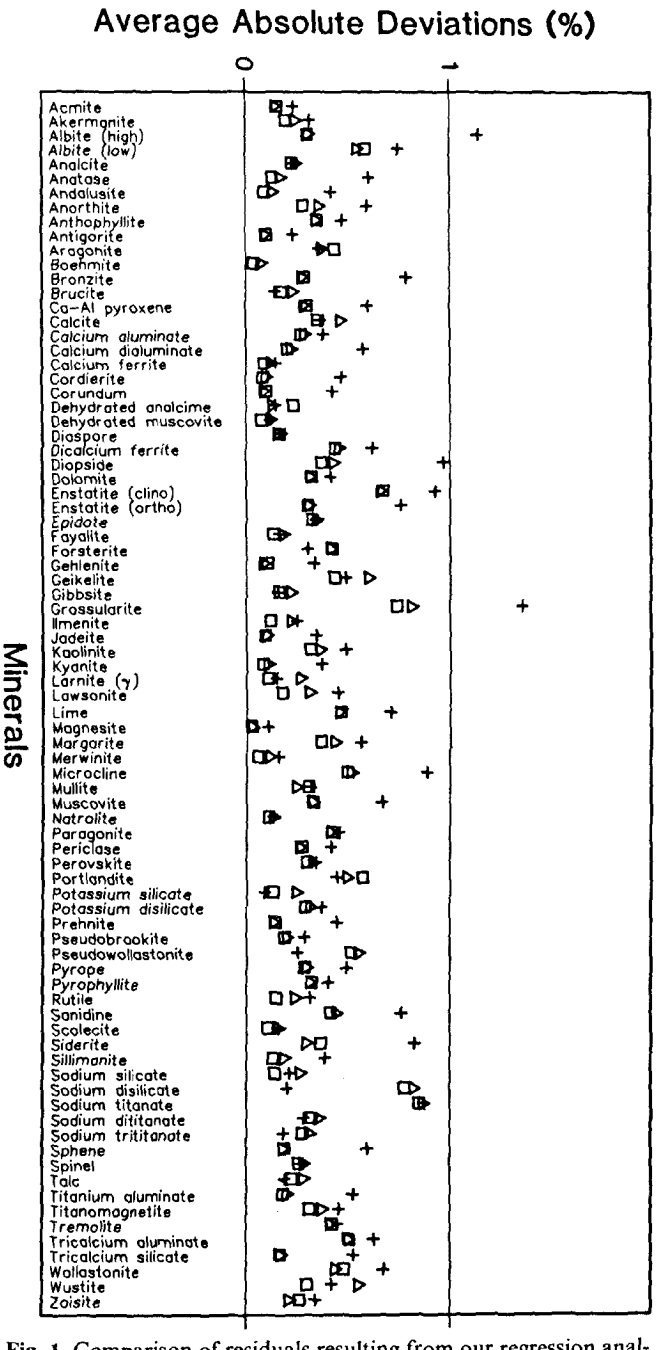

Fig. 1. Comparison of residuals resulting from our regression analysis of calorimetric data with the Maier-Kelley equation (*crosses*), the Haas-Fisher equation (*squares*), and with equation 7 (*triangles*). Residuals for each mineral calculated as average absolute percent deviations of the fitted function from the data. Data below 300 K were not included in the regression analysis using the MK equation

Evaluation of the quality of data representation with equation 7 must assess both the magnitude of regression residuals and the trend of residuals as a function of temperature. For most minerals, the magnitudes of average absolute deviations calculated with equation 7 are slightly greater (<0.1%) than those resulting from analysis of the same data using the HF equation (Fig. 1). Residuals are significantly greater (more than twice) than those calculated with the HF equation for 6 of 85 phases (geikelite, ilmenite, γ-larnite, sodium silicate, potassium silicate, and wustite)

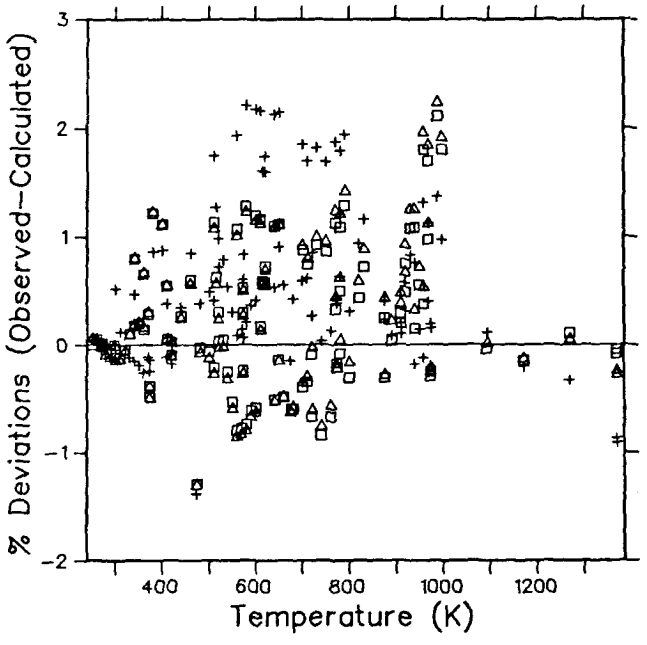

Fig. 2. Percent differences between heat capacity and heat content data for low albite (references given in Table 3) and values derived by regression analysis with the MK equation (*crosses*), the HF equation (*squares*), and with equation 7 (*triangles*). Note the random distribution of residuals produced with the latter two equations for the C_P data up to about 850 K. Above this temperature the precision of these data rapidly decreases (Krupka et al. 1985b; Mraw and Naas, 1979). The smaller magnitude of residuals below 300 K reflect the greater weight given to the more accurate adiabatic calorimetry data (see Appendix 1)

for which data are available above 298.15 K (Fig. 1). However, for ony two minerals (geikelite and wustite), are the average absolute deviations unacceptably large compared to the estimated uncertainties of the measurements, and these cases reflect poor agreement between low and high temperature data sets. Even when data below 300 K are excluded from the analysis, use of the MK equation frequently leads to residuals which are substantially greater than those calculated with the HF equation or with equation 7 (Fig. 1).

For the majority of minerals, residuals (measured – fit C_P) are randomly distributed as a function of temperature, and, as shown for the data of low albite (Fig. 2), are quite similar to those resulting from analysis with the HF equation. Residuals computed with the MK equation, however, are systematically high at low temperatures and low at high temperatures, invariably leading to overestimates of heat capacities at high temperatures. Non-random distributions of residuals are produced with equation 7 in cases where low temperature adiabatic calorimetric data are in poor agreement with data at higher temperatures, as discussed above. In such cases the ability to extrapolate beyond the data with equation 7 sacrifices the improved representation of combined data sets obtained with the HF equation.

Although the maximum temperature of calorimetric measurements on most minerals is in the range 1,000–1,800 K, analysis of available C_P data for minerals with equation 7 results in high temperature heat capacities which are remarkably consistent on an atomic basis. The average C_P at 3,000 K for 91 minerals for which calorimetric data above 400 K have been obtained is 28.3±2.0 J/

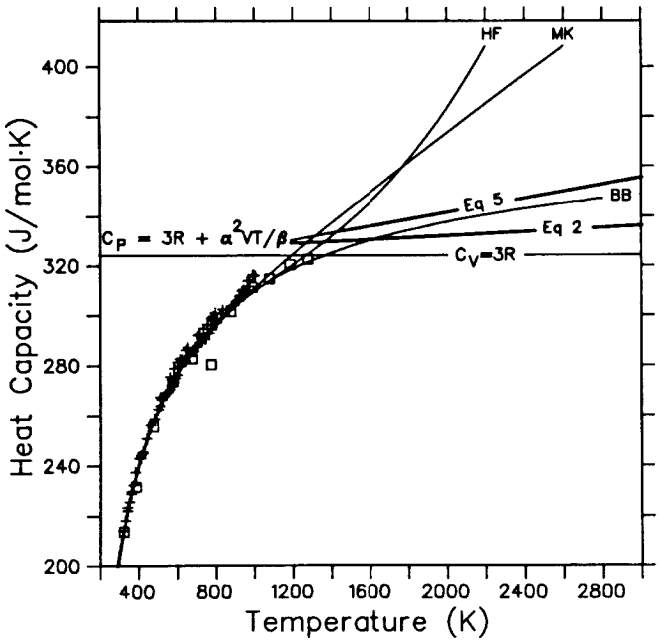

Fig. 3. Comparison of the temperature dependence of the heat capacity of low albite resulting from our regression analysis of calorimetric data with the Maier-Kelley (MK) equation, the Haas-Fisher (HF) equation, and with equation 7 (BB). Note that only the curve fit with equation 7 is in accord with the high temperature heat capacities predicted theoretically with equations 2 and 5. Sources of adiabatic calorimetry data (*crosses*) and drop calorimetry data (*finite difference derivatives shown as squares*) are given in Table 3

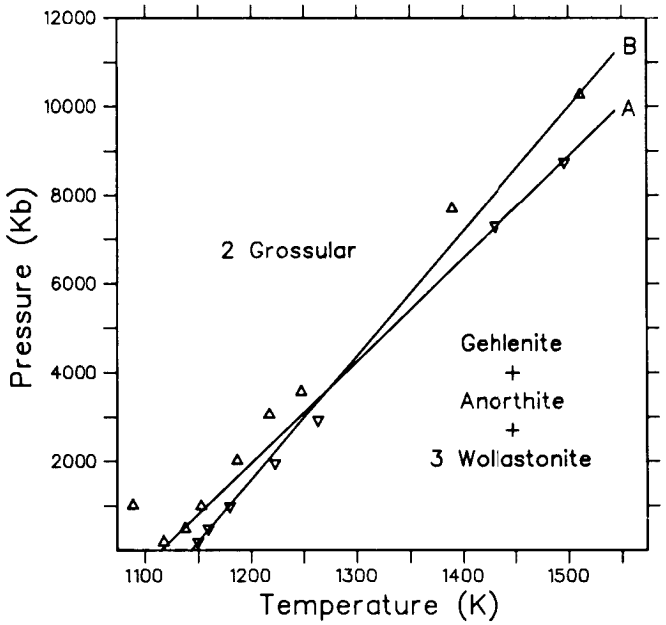

Fig. 4. Phase equilibria data of Huckenholz et al. (1975) used to derive the third law entropy of grossular. See text for discussion

(afu·K). This value is in good agreement with the range of average values ($26.8 \pm 0.8 - 29.3 \pm 1.9$ J/(afu·K)) derived theoretically with equations 2 and 5, as discussed above. Although heat capacities calculated with the coefficients in Table 3 are used most confidently within the range of the data shown, the above comparison suggests that extrapolation to considerably higher temperatures should be reliable.

A representative example of the differences in the variation of C_P with T produced with the different empirical equations is shown in Fig. 3. The three different C_P equations all reproduce the calorimetric data for albite within reasonable limits, but they diverge markedly at temperatures higher than the experimental data. Only equation 7 yields a C_P versus T curve which is in accord with the theoretically derived limit for C_P at high temperature. We reiterate, however, that the MK and HF equations were never intended to be used for the purpose of extrapolation without additional constraints to high temperature C_P, and we show the above comparison solely to reinforce this point.

Although we are rarely interested in heat capacity at temperatures as high as 3,000 K, the large differences in extrapolated heat capacity at this temperature (Fig. 3) emphasize the importance of correct limiting C_P behavior for calculations of the C_p of minerals involved in high temperature processes, most notably melting phenomena. While not as pronounced, the differences at 3,000 K alluded to above also reflect significant differences in heat capacity at lower temperatures of more general geologic interest.

We illustrate this point by deriving the third law entropy of grossular at 298.15 K from experimental data between 1,100 and 1,500 K for the equilibrium grossular = anorthite + 3 wollastonite + gehlenite. Note that the heat capacity of grossular has been measured only up to 1,273 K (Table 3). For the purpose of these calculations, volumes of all phases were taken from Robie et al. (1967), and the third law entropies of wollastonite, gehlenite, and anorthite were taken from the data of Krupka et al. (1984a), Waldbaum (1973), and Robie et al. (1978), respectively. Both of the curves shown in Fig. 4 can be calculated using he. capacities for all phases fit with either the MK or our equation, but the resulting entropy of grossular varies by approximately 4.5 J/mole depending on which C_P equation is used. Comparison is not made with the HF equation because additional constraints are needed to force smooth extrapolations with this equation. The range of entropy values permitted by the reversals (corresponding to the minimum (A) and maximum (B) $P-T$ slopes of the equilibrium) are 230.7–251.1 J/mole using the MK equation, and 235.3 – 255.5 J/mole using our equation. Calorimetric data yield third law entropies at 298.15 K ranging from 254.72 J/mole (Westrum et al. 1979) to 260.12 J/mole (Haselton and Westrum 1980), and give support to the results obtained with our revised C_P equation.

We emphasize that these differences in the derived third law entropy of grossular result largely from the extrapolation of its heat capacity above the temperatures (1,273 K) of the calorimetric data. Similar differences are obtained when the calculations are repeated using C_P's of other phases in this equilibrium which are represented with equation 7. As these calculations indicate, derivation of standard state entropies (or the entropy effects of disordering phenomena) from phase equilibria data are highly dependent on the nature of C_P extrapolations.

Heat capacity estimation

Several methods have been proposed for estimation of the heat capacity of minerals for which calorimetric data have not be measured. The simplest approach for silicates, for

Table 4. Coefficients for heat capacity (J/mol·K) estimation, calculated from weighted linear regression of data on Table 3

	k_0	$k_1 \times 10^{-2}$	$k_2 \times 10^{-5}$	$k_3 \times 10^{-7}$
Na_2O	95.148	0.0	−51.0405	83.3648
K_2O	105.140	−5.7735	0.0	0.0
CaO	60.395	−2.3629	0.0	−9.3493
MgO	58.196	−1.6114	−14.0458	11.2673
FeO	77.036	−5.8471	0.0	0.5558
Fe_2O_3	168.211	−9.7572	0.0	−17.3034
TiO_2	85.059	−2.2072	−22.5138	22.4979
SiO_2	87.781	−5.0259	−25.2856	36.3707
Al_2O_3	155.390	−8.5229	−46.9130	64.0084
H_2O (structural)	106.330	−12.4322	0.0	9.0628
H_2O (zeolitic)	87.617	−7.5814	0.0	0.5291
CO_2	119.626	−15.0627	0.0	17.3869

example, involves summation of the heat capacities of single oxide minerals in the proportions in which they occur in the mineral. This method generally yields heat capacities estimated to be accurate within 5% (Helgeson et al. 1978). Helgeson et al. (1978) proposed an alternative method for heat capacity estimation (within 2%) in which they consider that $\Delta C_P = 0$ for exchange reactions involving structurally similar compounds. As pointed out by Robinson and Haas (1983), this technique is path-dependent, and very different C_P values can result from use of different exchange reactions. These authors in turn estimate heat capacity (within 2%) from regression of C_P data with the model

$$C_P(A) = \sum_i n_i c_i^* \tag{10}$$

where n_i and c_i^* are the number of moles and the regressed C_P function (using the HF equation), respectively, of the i-th component of phase A. Robinson and Haas give heat capacity functions for 23 'components' which account for various coordination states of cations in common minerals.

Because C_P in minerals arises largely from vibration of atoms within the crystalline lattice, one might expect heat capacity to depend on cation coordination. Although provision for different cation coordinations has important effects on entropy prediction, we have found that providing for different coordination states results in insignificant (e.g. <2% for the aluminosilicates) improvements to the overall representation of high temperature heat capacity data (with the exception of hydrous phases discussed below) when compared to the model:

$$C_P(A) = \sum_i n_i c_i^* \tag{11}$$

where n_i and c_i^* are the number of moles and the regressed C_P function (using equation 7), respectively, of the i-th *oxide* component of phase A. The main advantage of this model over that proposed by Robinson and Haas (1983) is that knowledge of cation coordinations in mineral structures is unnecessary for heat capacity estimation.

Table 4 presents the coefficients which allow estimation of the heat capacity of minerals with equation 11. These coefficients were determined by weighted linear regression (see Appendix 1 for details) of all calorimetric data above 250 K for the minerals listed in Table 3, with the exception of those phases which undergo lambda transitions. In addition, unpublished calorimetric data above 298 K were included for ferrosilite, ilmenite, and almandine (L. Anovitz) and for grunerite (B.S. Hemingway). For most minerals, average residuals of this fit are less than 2% (Fig. 5), and are similar in magnitude to residuals obtained with the model of Robinson and Haas (1983).

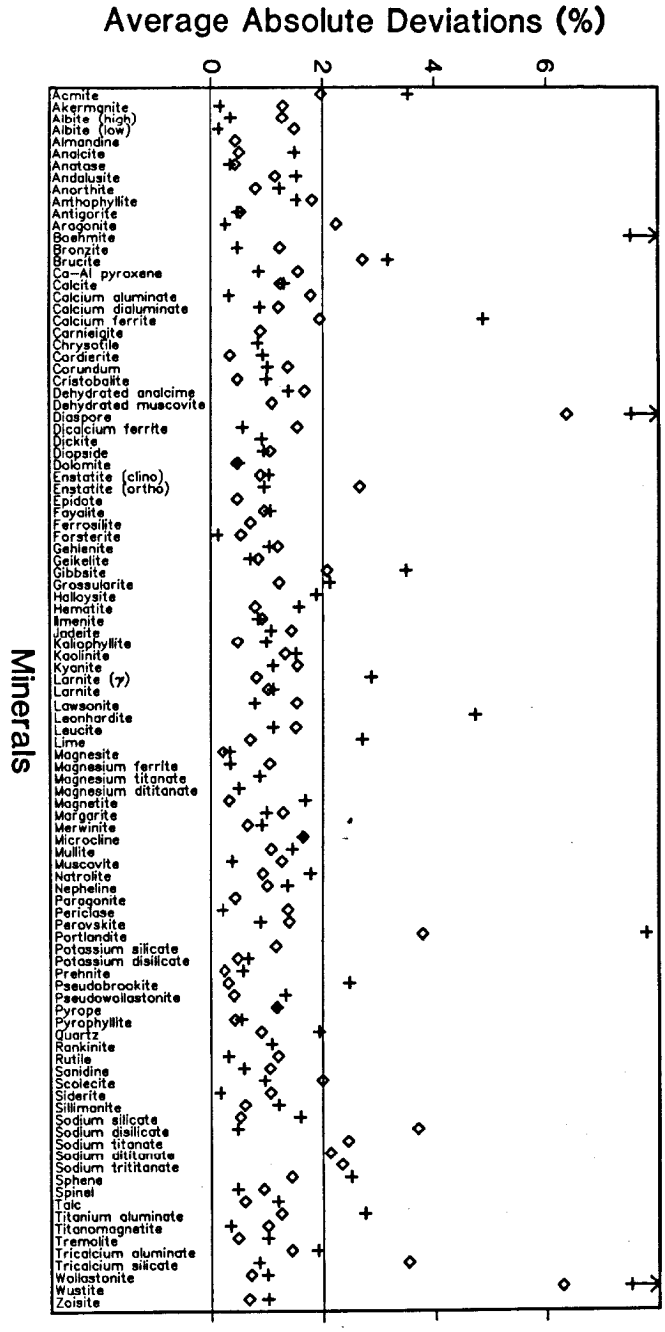

Fig. 5. Regression residuals of estimated heat capacities using equation 11. Residuals are calculated as average absolute percent deviations of the estimated heat capacities from the low temperature adiabatic calorimetric (*crosses*) and high temperature (*diamonds*) data listed in Table 3. Calorimetric data in the temperature range of any lambda transitions were omitted from the calculations

Most of the phases which show the largest residuals are hydrous minerals. Attempts were made to improve the results by accounting for the differences in the nature of the hydrogen bonding in these phases. Separation of the C_P contribution of H_2O into 'structural' and 'zeolitic' components led to significant improvements, and thus we have

Table 5: Comparison between heat capacities estimated with equation 11 and calorimetric data not used to derive Table 4 coefficients

Mineral	Composition	Range (K)	AAD[a]	Reference
Amosite	$Fe^{2}_{5.28}Fe^{3}_{0.12}Mg_{1.52}Mn_{0.08}Si_{7.92}Al_{0.08}O_{22.04}(OH)_{1.96}$	257– 852	0.83	Bennington et al. (1978)
Andradite	$Ca_{2.94}Mn_{0.04}Fe^{2}_{0.01}Fe^{3}_{1.77}Al_{0.29}Si_{2.96}Ti_{0.01}O_{12}$	335-1100	1.85	Kiseleva et al. (1972)
Chlorite	$Mg_{3.52}Mn_{0.01}Fe^{2}_{0.57}Fe^{3}_{0.21}Al_{2.40}Si_{2.99}O_{10}(OH)_{8}$	51– 500	0.78	Hemingway et al. (1984)
Clinochlore	$Na_{0.03}Mg_{4.7}Fe^{2}_{0.14}Fe^{3}_{0.04}Cr_{0.16}Al_{2.02}Si_{2.91}O_{10.01}(OH)_{7.99}$	400– 800	1.60	Henderson et al. (1983)
Clinozoisite	$Ca_{1.82}Sr_{0.08}Na_{0.01}Mg_{0.03}Fe^{2}_{0.05}Fe^{3}_{0.35}Al_{2.64}Ti_{0.01}Si_{3}O_{12}(OH)_{0.99}$	335–1100	1.35	Kiseleva et al. (1974)
Crocidolite	$Na_{1.9}Ca_{0.1}Fe^{2}_{2.5}Fe^{3}_{2.02}Mg_{0.48}Al_{0.03}Si_{7.97}O_{22.1}(OH)_{1.91}$	259– 902	1.74	Bennington et al. (1978)
Grunerite	$Fe^{2}_{6.1}Mg_{0.8}Mn_{0.08}Ca_{0.02}Si_{8}O_{22}(OH)_{2}$	30–1000	1.49	Hemingway (unpublished)
Hedenbergite	$Ca_{0.95}Fe^{2}_{0.71}Fe^{3}_{0.09}Mg_{0.06}Mn_{0.14}Si_{2}O_{6}$	253–1147	1.48	Bennington et al. (1984)
Monticellite	$Ca_{0.99}Mg_{0.93}Mn_{0.01}Fe^{2}_{0.08}Si_{0.98}O_{3.98}$	300–1000	0.77	Sharp et al. (1983)
Osumilite	$K_{0.93}Na_{0.09}Ca_{0.02}Ba_{0.01}Mg_{1.88}Fe^{2}_{0.38}Ti_{0.01}Al_{4.62}Si_{10.1}O_{30}$	40– 998	0.68	Hemingway et al. (1984)
Pyrope	$Mg_{2.15}Fe^{2}_{0.48}Fe^{3}_{0.01}Mn_{0.03}Ca_{0.43}Al_{1.85}Cr_{0.06}Si_{2.99}Ti_{0.02}O_{12}$	335–1000	1.00	Kiseleva et al. (1972)
Staurolite	$Al_{8.89}Mg_{0.22}Fe^{2}_{2.7}Fe^{3}_{0.27}Mn_{0.01}Ti_{0.04}Si_{4.02}O_{23.45}(OH)_{1.5}$	255– 889	1.97	Hemingway and Robie (1984a)

[a]Average absolute deviation (%) of estimated heat capacities from data

retained both H_2O components for estimation of the heat capacity of hydrous minerals. Further separation of the 'structural' H_2O component into a 'brucite' and 'pyrophyllite' coordination-type did not result in significantly lower residuals.

With the exception of data for diaspore, portlandite, and boehmite, the model accounts satisfactorily for the data for minerals containing structural H_2O, and marked inconsistencies between low and high temperature data for the latter two phases suggests that the large residuals may, to a certain extent, reflect inaccurate calorimetric data. The same argument may apply to the high temperature data for sodium disilicate (Naylor 1945a) and the sodium-titanates (Naylor 1945b) because recent data of Richet et al. (1984) for sodium silicate are systematically lower by about 2% than the data for this phase reported by Naylor (1945a). Although calorimetric data above 298 K for zeolites are reproduced adequately, estimated values between 250–300 K for analcite, natrolite, and leonhardite (Table 3, Fig. 5), and for phillipsite and clinoptilolite (Hemingway and Robie 1984b) show large discrepancies. Significant differences observed in the heat capacity and entropy contribution of zeolitic water between different zeolites (Johnson et al. 1983; Hemingway and Robie 1984b) suggests that additional zeolitic H_2O components will be necessary in order to predict accurately low temperature heat capacities for zeolites.

An important test of this model is to compare estimated heat capacities of minerals with experimental data that were not used to determine the coefficients of Table 4. Calorimetric data for the phases shown in Table 5 were not used in the regression analysis because of the presence in these phases of MnO, SrO, ZnO, and Cr_2O_3, components that were not considered in the present study. Heat capacities for these samples are calculated by summation of the C_P coefficients of the oxide components (Table 4) in the proportions given by the mineral formulas in Table 5 (note that $Na = Na_2O/2$, $K = K_2O/2$, $Fe^3 = Fe_2O_3/2$, $Al = Al_2O_3/2$, $OH = H_2O/2$). For the purposes of these calculations, the C_P contributions of MnO, SrO, ZnO and Cr_2O_3 were calculated from data tabulated by Kelley (1960). As indicated in Table 5, our C_P estimates for these phases are in good agreement with the experimental data, and support our contention that the proposed estimation technique yields high temperature C_P of minerals reliable to within 2%.

In addition to yielding estimated heat capacities of minerals, the coefficients given in Table 4 can be used to correct high temperature C_P data for the effects of sample impurities, although this technique will be more powerful when the predictive model is extended to other components present in naturally occurring minerals. Because estimated heat capacities are reliable within 2%, correction of calorimetric data for a sample which deviates from end-member stoichiometry by 10% should introduce errors no greater than 0.2%. This procedure offers an alternative to correction techniques based on measured heat capacities of other minerals (e.g. Westrum et al. 1979).

Conclusions

The revised heat capacity equation proposed in this paper reproduces calorimetric data for minerals more closely than the MK equation, and nearly as well as the HF equation. When compared to the estimated precision of the calorimetric data, the differences with the latter equation are insignificant for most minerals. The most important advantage of the revised C_P equation is that it allows for reliable extrapolation to high temperatures.

The revised heat capacity equation should improve thermodynamic calculations involving minerals at temperatures higher than those of available calorimetric data. Two examples may serve to illustrate this point: (a) Use of equation 7 allows for the derivation of standard state thermochemical properties of minerals in the system $Na_2O-K_2O-CaO-MgO-FeO-Fe_2O_3-Al_2O_3-SiO_2-TiO_2-H_2O-CO_2$ that are consistent with available phase equilibrium, calorimetric, and volumetric data (Berman et al. 1984). (b) Because extrapolations of the C_P of minerals with different functions increasingly diverge as temperatures increase above available data (see Fig. 3), use of equation 7 has very important effects on the calculation of high temperature processes such as mineral-melt equilibria (Ghiorso et al. 1983; Berman and Brown 1984), although more work is necessary to constrain the C_P of the melt phase (Stebbins et al. 1984; Richet and Bottinga 1982).

C_P coefficients of 'oxide components' given in Table 4 allow for the estimation of the heat capacity of minerals within approximately 2%. These predictions provide the means for extending thermodynamic analysis to a greater number of minerals than previously possible. In addition, use of the heat capacities of the oxide components provides

a convenient method for correction of calorimetric data above 298 K for the effects of sample impurities.

Appendix 1: Procedures for analysis of calorimetric data

We present in Table 3 C_P coefficients for minerals in the system $Na_2O-K_2O-CaO-MgO-FeO-Fe_2O_3-Al_2O_3-SiO_2-TiO_2-H_2O-CO_2$. Selection among alternate data sets for a given mineral was based primarily on precision of data, and on the proximity of sample compositions to end-member stoichiometry, with preference given to synthetic minerals. Where multiple data sets were available, and provided that the above conditions were satisfied, we favored those sets which gave best agreement in the temperature range of overlap of different data sets.

The temperature dependence of the heat capacity of minerals is determined primarily by three experimental methods. Direct measurements of C_P are available at low temperatures from adiabatic calorimetry which yields results generally precise to 0.1% and accurate to 0.1–0.3% (Kelley et al. 1946; Robie et al. 1982b). At higher temperatures, up to 1,000 K, C_P can be measured directly by differential scanning calorimetry (DSC). Results are commonly reported to be precise to 0.3–1.0% and accurate to within 1.0% (O'Neill 1966; Krupka et al. 1979; Perkins et al. 1980), although the work of Mraw and Naas (1979) indicates uncertainties up to 2% at temperatures above about 800 K. Alternately, high temperature heat capacities can be derived by drop calorimetry which measures the enthalpy differences between high temperatures and the reference temperature. Because $C_P=(\partial H/\partial T)_P$, C_P can be derived by fitting the drop calorimetric data to the integrated form of equation 7

$$H_T-H_{T_r}=k_0(T-T_r)+2k_1(T^{0.5}-T_r^{0.5})-k_2(T^{-1}-T_r^{-1}) -0.5k_3(T^{-2}-T_r^{-2}) \quad (A1)$$

where T_r is the reference temperature of the experiments. The precision of drop calorimetric data is 0.1–0.2%, and absolute uncertainties in heat contents are estimated at 0.2–0.4% (Kelley et al. 1946; Victor and Douglas 1963; Ko et al. 1977; Richet et al. 1982).

Several authors (e.g. Maier and Kelley 1932; Richet et al. 1982) use an alternate form of the integrated C_P equation for analysis of heat content data. Applied to our equation, their model leads to

$$H_T-H_{T_r}=k_0\,T+2k_1\,T^{0.5}-k_2\,T^{-1}-0.5k_3\,T^{-2}+k_4 \quad (A2)$$

which is equivalent to equation A1 only if

$$k_4=(-k_0\,T_r-2k_1\,T_r^{0.5}+k_2\,T_r^{-1}+0.5\,k_3\,T_r^{-2})$$

Use of equation A2 results in lower residuals than equation A1 because of the extra degree of freedom gained by not forcing T_r to be equal to the reference temperature of the experiments, or conversely, by not ensuring that

$$H_T-H_{T_r}=0 \quad (A3)$$

when $T=T_r$. Thermodynamic calculations require that equation A3 be satisfied, and thus C_P coefficients derived by using equation A2 will lead to $(H_T-H_{T_r})$ values which are displaced by a constant equal to

$$(k_4+k_0\,T_r+2k_1\,T_r^{0.5}-k_2\,T_r^{-1}-0.5k_3\,T_r^{-2}).$$

Because of this inconsistency, we recommend that equation A2 not be used.

Data from the three sources discussed above are fit simultaneously (equations 7 and A1) using a linear regression package (BMDP statistical software, program P3R, University of California at Los Angeles), which allows k_1 and k_2 of equations 7 and A1 to be constrained to be negative. In cases where either coefficient is zero in Table 3, lower residuals could have been obtained by permitting the coefficient to be positive. All data are weighted by either $1/(p(H_T-H_{T_r}))^2$ or $1/(p(C_P))^2$, where p is the precision of measurement. The values used for p are 0.1% for adiabatic calorimetric data, 0.2% for drop calorimetric data, 1.0% for DSC data. In addition to weighting the fit towards the more precise data, this procedure provides a means for balancing the weight given to (1) different types of data, because C_P and heat content values commonly differ by an order of magnitude, and (2) high and low temperature data which also show a large variation in absolute magnitude (particularly heat content data). Because we are interested primarily in heat capacity above 298.15 K, we incorporate adiabatic calorimetric data only above approximately 250 K, even where data are available at lower temperatures. Use of these data ensures that the high temperature C_P function joins smoothly with the more accurate adiabatic calorimetric data which provide important constaints on the slope of the C_P function at temperatures above 298.15 K.

For cases in which preliminary analysis indicates poor agreement between low and high temperature data sets, three alternate strategies are used to improve overall data representation: 1) weighting factors are adjusted to give more weight to the higher temperature data, 2) C_P data at the lowest temperatures (near 250 K) are removed, or 3) relative enthalpy data just above 298 K are given less weight so as to yield better data representation of C_P data at high temperatures.

Coefficients for heat capacity estimation with equation 11 are derived by analysis of all calorimetric data for the minerals listed in Table 3, with the exception of those phases which undergo lambda transitions. In addition, we included unpublished data above 298.15 K for almandine, ferrosilite, and ilmenite (L. Anovitz) and for grunerite (B.S. Hemingway). Weighting factors, calculated as described above, were modified by 1) normalizing all mineral formulae to an equal oxygen basis, and 2) counter-balancing the large amount of data for phases composed of CaO, MgO, Al_2O_3, and SiO_2 by increasing weighting factors by a factor of 2 for minerals containing Na_2O, K_2O, FeO, Fe_2O_3, TiO_2, CO_2, or zeolitic H_2O.

Appendix 2: Calculation of the thermodynamic properties of phases which undergo lambda transitions

At any pressure, P, the temperature of a polymorphic transition, T_λ^P, can be represented by

$$T_\lambda^P=T_\lambda^{1\ bar}+(\partial T/\partial P)_G\cdot(P-1)$$

where $T_\lambda^{1\ bar}$ is the transition temperature at 1 bar. T_d is defined as the difference in transition temperatures between 1 bar and pressure, P, so that $T_d=T_\lambda^{1\ bar}-T_\lambda^P$. The contribution to the CP arising from the lambda transition, C_{P_λ}, is assumed to be constant at all pressures, and is computed from

$$C_{P_\lambda}=t'(l_1+l_2t')^2 \quad (A4)$$

where $t'=T+T_d$. If we similarly define a reference temperature, $t_r=T_{ref}-T_d$, equation A1 can be integrated to give the change in enthalpy and entropy due to the lambda transition:

$$\Delta H_\lambda=\int_{t_r}^{T} CP_\lambda dT=H_T-H_{t_r}=x_1(T-t_r)+x_2(T^2-t_r^2)/2 +x_3(T^3-t_r^3)/3+x_4(T^4-t_r^4)/4 \quad (A5)$$

$$\Delta S_\lambda=\int_{t_r}^{T}(CP_\lambda/T)dT=S_T-S_{t_r}=x_1(\ln(T)-\ln(t_r)) +x_2(T-t_r)+x_3(T^2-t_r^2)/2+x_4(T^3-t_r^3)/3 \quad (A6)$$

where

$$x_1=l_1^2T_d+2l_1l_2T_d^2+l_2^2T_d^3$$
$$x_2=l_1^2+4l_1l_2T_d+3l_2^2T_d^2$$
$$x_3=\partial l_1l_2+3l_2^2T_d$$
$$x_4=l_2^2$$

Note that if T is greater than the transition temperature, T_λ^P, the integration is performed between t_r and T_λ^P. The change in Gibbs free energy contributed by the increase in heat capacity associated with the lambda transition is calculated from

$$\Delta G_\lambda = \Delta H_\lambda - T \cdot \Delta S_\lambda$$

Acknowledgements. The work reported in this paper could not have been attempted without the compilation and organization of the large amount of C_P data determined over the past sixty-five years. We are indebted to J. Rulon, K. Parrish, M. St. Pierre, and M. Piranian for their efforts in gathering and organizing these data, and for their patience in laboring through the seemingly endless attempts to fit them. We also wish to extend our gratitude to L. Anovitz, H.T. Haselton, B.S. Hemingway, T.J. Holland, K.M. Krupka, and D. Perkins III, for providing us with valuable unpublished data.

We are most grateful to Martin Engi for many helpful suggestions and discussions at various stages in the course of this work. We also thank Martin Engi, Bear McPhail, T.T. Vandergraaf, N.C. Garisto, M. Ghiorso, R.J. Lemire, and V.N. Fleer for their careful reviews of an early version of this manuscript. In addition, we are most appreciative of the thoughtful comments provided by K. Krupka, P. Richet, and an anonomous reviewer, all of which led to a greatly improved manuscript. This research was funded by Atomic Energy of Canada, Ltd. (Geochemistry and Applied Chemistry Branch, Waste Management Division) through contract A-7436/R1.

References

Anderson CT (1934) The heat capacities of magnesium, zinc, lead, manganese and iron carbonates at low temperatures. J Am Chem Soc 56:849–851

Anderson CT (1936) The heat capacities of quartz, cristobalite and tridymite at low temperatures. J Am Chem Soc 58:568–570

Barron THK, Berg WT, Morrison JA (1959) On the heat capacity of crystalline magnesium oxide. Proc R Soc London A250:70–83

Bennington KO, Ferrante MJ, Stuve JM (1978) Thermodynamic data on the amphibole asbestos minerals amosite and crocidolite. US Bur Mines Rep Inv 8265:30p

Bennington KO, Beyer RP, Brown RR (1984) Thermodynamic properties of hedenbergite, a complex silicate of Ca, Fe, Mn, and Mg. US Bur Mines Rep Inv 8873:19p

Berman RG, Brown TH (1983) A revised equation for representation and high temperature extrapolation of the heat capacity of minerals. EOS 64:875

Berman RG, Brown TH (1984) A thermodynamic model for multicomponent melts, with application to the system $CaO-Al_2O_3-SiO_2$. Geochim Cosmochim Acta 45:661–678

Berman RG, Brown TH, Engi M (1984) A thermodynamic data base for minerals: I. A linear programming analysis of experimental data in a ten component system. Proc IUPAC Conf Chem Therm: paper 180

Beyer RP, Ferrante MJ, Brown RR, Daut GE (1980) Thermodynamic properties of potassium metasilicate and disilicate. US Bur Mines Rep Inv 8410:21p

Birch F (1966) Compressibility; elastic constants. In: Clark SP (ed) Handbook of Physical Constants, Geol Soc Am Mem 97:97–173

Boltzmann L (1871) Einige allgemeine Sätze über Wärmegleichgewicht. Sitzungsber K Akad Wiss Wien 63:679–711

Bonnickson KR (1954) High-temperature heat contents of calcium and magnesium ferrites. Am Chem Soc J 76:1480–1482

Bonnickson KR (1955a) High temperature heat contents of aluminates of calcium and magnesium. J Phys Chem 59:220–221

Bonnickson KR (1955b) High temperature heat contents of some titanates of aluminum, iron and zinc. Am Chem Soc J 77:2152–2154

Coughlin JP, King EG, Bonnickson KR (1951) High-temperature heat contents of ferrous oxide, magnetite and ferric oxide. Am Chem Soc J 73:3891–3893

Coughlin JP, O'Brien CJ (1957) High temperature heat contents of calcium orthosilicate. J Phys Chem 61:767–769

Debye P (1912) Zur Theorie der spezifischen Wärmen. Ann Phys 39:789–839

Ditmars DA, Douglas TB (1971) Measurement of the relative enthalpy of pure $\alpha-Al_2O_3$ (NBS heat capacity and enthalpy standard reference material no. 720) from 273 to 1,173 K. J Res Nat Bur Stand 75A:401–420

Einstein A (1907) Die Plancksche Theorie der Strahlung und die Theorie der spezifischen Wärme. Ann Phys 22:180–190

Elsner von Gronow H, Schwiete HE (1933) Die spezifischen Wärmen von CaO, Al_2O_3, $CaO \cdot Al_2O_3$, $3CaO \cdot Al_2O_3$, $2CaO \cdot SiO_2$, $3CaO \cdot SiO_2$, $2CaO \cdot Al_2O_3 \cdot SiO_2$ von 20 bis 1,500 C. Z Anorg Allg Chem 216:185–195

Ghiorso MS, Carmichael ISE, Moret LK (1979) Inverted high-temperature quartz. Unit cell parameters and properties of the alpha-beta inversion. Contrib Mineral Petrol 68:307–323

Ghiorso MS, Carmichael ISE, Rivers ML, Sack RO (1983) The Gibbs free energy of mixing of natural silicate liquids: an expanded regular solution approximation for the calculation of magmatic intensive variables. Contrib Mineral Petrol 84:107–145

Giauque WF, Archibald RC (1937) The entropy of water from the third law of thermodynamics. The dissociation pressure and calorimetric heat of the reaction $Mg(OH)_2 = MgO + H_2O$. The heat capacities of $Mg(OH)_2$ and MgO from 20 to 300 K. Am Chem Soc J 59:561–569

Gmelin E (1969) Thermal properties of alkaline-earth-oxides. Z Naturforsch 24A:1794–1800

Gronvold F, Samuelson EJ (1975) Heat capacity and thermodynamic properties of $\alpha-Fe_2O_3$ in the region 300–1,050 K. J Phys Chem Solids 36:249–256

Gronvold F, Sveen A (1974) Heat capacity and thermodynamic properties of synthetic magnetite (Fe_3O_4) from 300 to 1,050 K. Ferrimagnetic transition and zero-point entropy. J Chem Thermodyn 6:859–872

Gronvold F, Westrum EF Jr (1959) α-ferric oxide: low temperature heat capacity and thermodynamic functions. Am Chem Soc J 81:1780–1783

Haas JL Jr, Fisher JR (1976) Simultaneous evaluation and correlation of thermodynamic data. Am J Sci 276:525–545

Haas JL Jr, Robinson GR Jr, Hemingway BS (1981) Thermodynamic tabulations for selected phases in the system $CaO-Al_2O_3-SiO_2-H_2O$ at 101.325 kPa (1 atm) between 273.15 and 1,800 K. J Phys Chem Ref Data 10:576–669

Haselton HT Jr (1979) Calorimetry of synthetic pyrope-grossular garnets and calculated stability relations. Doctoral Thesis, University of Chicago

Haselton HT Jr, Hemingway BS, Robie RA (1984) Low-temperature heat capacities of $CaAl_2SiO_6$ glass and pyroxene and thermal expansion of $CaAl_2SiO_6$ pyroxene. Am Mineral 69:481–489

Haselton HT Jr, Hovis GL, Hemingway BS, Robie RA (1983) Calorimetric investigation of the excess entropy of mixing in analbite-sanidine solid solutions: lack of evidence for Na, K short-range order and implications for two-feldspar thermometry. Am Mineral 68:398–413

Haselton HT Jr, Westrum EF Jr (1980) Low-temperature heat capacities of synthetic pyrope, grossular, and $pyrope_{60}grossular_{40}$. Geochim Cosmochim Acta 44:701–709

Hatton WE, Hildenbrand DL, Sinke GC, Stull DR (1959) The chemical thermodynamic properties of calcium hydroxide. Am Chem Soc J 81:5028–5030

Helgeson HC, Delaney JM, Nesbitt HW, Bird DK (1978) Summary and critique of the thermodynamic properties of rock-forming minerals. Am J Sci 278A:229p

Hemingway BS, Krupka KM, Robie RA (1981) Heat capacities of the alkali feldspars between 350 and 1,000 K from differential scanning calorimetry, the thermodynamic functions of the alkali feldspars from 298.15 to 1,400 K, and the reaction quartz + jadeite = analbite. Am Mineral 66:1202–1215

Hemingway BS, Robie RA (1984a) Heat capacity and thermodynamic functions for gehlenite and staurolite: with comments

on the Schottky anomaly in the heat capacity of staurolite. Am Mineral 69:307–318

Hemingway BS, Robie RA (1984b) Thermodynamic properties of zeolites: low-temperature heat capacities and thermodynamic functions for phillipsite and clinoptilolite. Estimates of the thermochemical properties of zeolitic water at low temperature. Am Mineral 69:692–700

Hemingway BS, Robie RA, Fisher JR, Wilson WH (1977) Heat capacities of gibbsite, $Al(OH)_3$, between 13 and 480 K and magnesite, $MgCO_3$, between 13 and 380 K and their standard entropies at 298.15 K and the heat capacities of calorimetry conference benzoic acid between 12 and 316 K. J Res USGS 5:797–806

Hemingway BS, Robie RA, Kittrick JA (1978) Revised values for the Gibbs free energy of formation of [$Al(OH)_4^-$aq], diaspore, boehmite and bayerite at 298.15 K and 1 bar, the thermodynamic properties of kaolinite to 800 K and 1 bar, and the heats of solution of several gibbsite samples. Geochim Cosmochim Acta 42:1533–1543

Hemingway BS, Robie RA, Kittrick JA, Grew ES, Nelen JA, London D (1984) The heat capacities of osumilite from 298.15 to 1,000 K, the thermodynamic properties of two natural chlorites to 500 K, and the thermodynamic properties of petalite to 1,800 K. Am Mineral 69:701–710

Henderson CE, Essene EJ, Anovitz LM, Westrum EF Jr, Hemingway BS, Bowman JR (1983) Thermodynamics and phase equilibria of clinochlore, $(Mg_5Al)(Si_3Al)O_{10}(OH)_8$. EOS 64:466

Holland TJB (1979) Experimental determination of the reaction paragonite = jadite + kyanite + H_2O, and internally consistant thermodynamic data for part of the system $Na_2O-Al_2O_3-SiO_2-H_2O$, with applications to eclogites and blueschists. Contrib Mineral Petrol 68:293–301

Holland TJB (1981) Thermodynamic analysis of simple mineral systems. In: Newton RC, Navrotsky A, Wood BJ (ed) Thermodynamics of Minerals and Melts. Springer Berlin Heidelberg New York, pp 19–34

Huckenholz HG, Holzl E, Lindhuber W (1975) Grossularite, its solidus and liguidus relations in the $CaO-Al_2O-SiO_2-H_2O$ system up to 10 kbar. Neues Jahrb Mineral Abh 124:1–46

Jacobs GK, Kerrick DM, Krupka KM (1981) The high temperature heat capacity of natural calcite ($CaCO_3$). Phys Chem Mineral 7:55–59

Johnson GK, Flotow HE, O'Hare PAG (1982) Thermodynamic studies of zeolites: analcime and dehydrated analcime. Am Mineral 67:736–748

Johnson GK, Flotow HE, O'Hare PAG (1983) Thermodynamic studies of zeolites: natrolite, mesolite and scolecite. Am Mineral 68:1134–1145

Kelley KK (1939) The specific heats at low temperatures of crystalline ortho-, meta-, and disilicates of sodium. Am Chem Soc J 61:471–473

Kelley KK (1943) Specific heats at low temperatures of magnesium orthosilicate and magnesium metasilicate. Am Chem Soc J 65:339–341

Kelley KK (1960) Contributions to the data on theoretical metallurgy. XIII. High-temperature heat-content, heat-capacity, and entropy data for the elements and inorganic compounds. US Bur Mines Bull 584:232p

Kelley KK, Naylor BF, Shomate CH (1946) Thermodynamic properties of manganese. US Bur Mines Tech Pap, 686:34p

Kelley KK, Todd SS, Orr RL, King EG, Bonnickson KR (1953) Thermodynamic properties of sodium-aluminum and potassium-aluminum silicates. US Bur Mines Rep Inv 4955, 21p

King EG (1954) Heat capacities at low temperatures and entropies at 298.16 K of calcium and magnesium ferrites. Am Chem Soc J 76:5849–5850

King EG (1955a) Heat capacities at low temperatures and entropies at 298.16 K of crystalline calcium and magnesium aluminates. J Phys Chem 59:218–219

King EG (1955b) Low-temperature heat capacties and entropies at 298.16 K of some titanates of aluminum, calcium, lithium and zinc. Am Chem Soc J 77:2150–2152

King EG (1957) Low temperature heat capacities and entropies at 298.15 K of some crystalline silicates containing calcium. Am Chem Soc J 79:5437–5438

King EG, Barany R, Weller WW, Pankratz LB (1967) Thermodynamic properties of forsterite and serpentine. US Bur Mines Rep Inv 6962:19p

King EG, Ferrante MJ, Pankratz LB (1975) Thermodynamic data for $Mg(OH)_2$ (brucite). US Bur Mines Rep Inv 8041:13p

King EG, Orr RL, Bonnickson KR (1954) Low temperature heat capacity, entropy at 298.16 K, and high temperature heat content of sphene ($CaTiSiO_5$). Am Chem Soc J 76:4320–4321

King EG, Weller WW (1961a) Low temperature heat capacities and entropies at 298.15 K of diaspore, kaolinite, dickite, and halloysite. US Bur Mines Rep Inv 5810:6p

King EG, Weller WW (1961b) Low temperature heat capacities and entropies at 298.15 K of some sodium- and calcium-aluminum silicates. US Bur Mines Rep Inv 5855:8p

Kiseleva IA, Topor ND, Andreyenko ED (1974) Thermodynamic parameters of minerals of the epidote group. Geochem Int 11:389–398

Kiseleva IA, Topor ND, Melchakova LV (1972) Experimental determination of heat content and heat capacity in grossular, andradite, and pyrope. Geokhimiya II:1372–1379

Ko HC, Ferrante MJ, Stuve JM (1977) Thermophysical properties of acmite. Proc 7th Symp Thermophys Properties. Am Soc Mech Eng:392–395

Kobayashi K (1950) The heat capacities of inorganic substances at high temperatures. Part II. The heat capacity of calcium hydroxide. Sci Rep Tohoku Univ 34:153–159

Kobayashi K (1951) The heat capacities of inorganic substances at high temperatures. Part IV: The heat capacity of synthetic aragonite (calcium carbonate). Sci Rep Tohoku Univ 35:111–118

Kolesnik YN, Nogteva VV, Arkhipenko DK, Orekhov BA, Paukov IY (1979) Thermodynamics of pyrope-grossular solid solutions and the specific heat of grossular at 13–300 K. Geochem Int 16:57–64

Krupka KM, Robie RA, Hemingway BS (1979) High-temperature heat capacities of corundum, periclase, anorthite, $CaAl_2Si_2O_8$ glass, muscovite, pyrophyllite, $KAlSi_3O_8$ glass, grossular, and $NaAlSi_3O_8$ glass. Am Mineral 64:86–101

Krupka MK, Robie RA, Hemingway BS, Kerrick DM, Ito J (1985a) Low-temperature heat capacities and derived thermodynamic properties of anthophyllite, diopside, enstatite, bronzite, and wollastonite. Am Mineral (in press)

Krupka MK, Robie RA, Hemingway BS, Kerrick DM, Ito J (1985b) High-temperature heat capacities and derived thermodynamic properties of anthophyllite, diopside, dolomite, enstatite, bronzite, talc, tremolite, and wollastonite. Am Mineral (in press)

Lander JJ (1951) Experimental heat contents of SrO, BaO, CaO, $BaCO_3$ and $SrCO_3$ at high temperatures. Dissociation pressures of $BaCO_3$ and $SrCO_3$. Am Chem Soc J 73:5794–5797

Lane DL, Ganguly J (1980) Al_2O_3 solubility in orthopyroxene in the system $MgO-Al_2O_3-SiO_2$: A reevaluation, and mantle geotherm. J Geophys Res 85:6963–6972

Maier CG, Kelley KK (1932) An equation for the representation of high temperature heat content data. Am Chem Soc J 54:3243–3246

Mraw SC, Naas DF (1979) The measurement of accurate heat capacities by differential scanning calorimetry. Comparison of DSC results on pyrite (100 to 800 K) with literature values from precision adiabatic calorimetry. J Chem Thermodyn 11:567–584

Naylor BF (1945a) High-temperature heat contents of sodium metasilicate and sodium disilicate. Am Chem Soc J 67:466–467

Naylor BF (1945b) High-temperature heat contents of Na_2TiO_3, $Na_2Ti_2O_5$ and $Na_2Ti_3O_7$. J Am Chem Soc 67:2120–2122

Naylor BF (1946) High-temperature heat contents of TiO, Ti_2O_3, Ti_3O_5, and TiO_2. Am Chem Soc J 68:1077–1080

Naylor BF, Cook OA (1946) High temperature heat contents of the metatitanites of calcium, iron, and magnesium. J Am Chem Soc 68:1003–1005

Newton RC, Thompson AB, Krupka KM (1979) Heat capacity of synthetic $Mg_3Al_2Si_3O_{12}$ from 350 to 1,000 K and the entropy of pyrope. EOS 58:523

O'Neill MJ (1966) Measurement of specific heat functions by differential scanning calorimetry. Anal Chem 38:1331–1336

Openshaw RE, Hemingway BS, Robie RA, Waldbaum DR, Krupka KM (1976) The heat capacity at low temperatures and entropies at 298.15 K of low albite, analbite, microcline, and sanidine. J Res USGS 4:195–204

Orr RL (1953) High temperature heat contents of magnesium orthosilicate and ferrous orthosilicate. Am Chem Soc J 75:528–529

Pankratz LB (1964) High-temperature heat contents and entropies of muscovite and dehydrated muscovite. US Bur Mines Rep Inv 6371:6p

Pankratz LB (1968) High-temperature heat contents and entropies of dehydrated analcite, kaliophilite, and leucite. US Bur Mines Rep Inv 7073:8p

Pankratz LB, Kelley KK (1963) Thermodynamic data for magnesium oxide (periclase). US Bur Mines Rep Inv 6295:5p

Pankratz LB, Kelley KK (1964a) High-temperature heat contents and entropies of andalusite, kyanite, and sillimanite. US Bur Mines Rep Inv 6370:7p

Pankratz LB, Kelley KK (1964b) High-temperature heat contents and entropies of akermanite, cordierite, gehlenite, and merwinite. US Bur Mines Rep Inv 6555:7p

Pankratz LB, Weller WW, Kelley KK (1963) Low-temperature heat capacity and high temperature heat content of mullite. US Bur Mines Rep Inv 6287:7p

Perkins D III, Essene EJ, Westrum EF Jr, Wall VJ (1979) New thermodynamic data for diaspore and their application to the system $Al_2O_3-SiO_2-H_2O$. Am Mineral 64:1080–1090

Perkins D III, Westrum EF Jr, Essene EJ (1980) The thermodynamic properties and phase relations of some minerals in the system $CaO-Al_2O_3-SiO_2-H_2O$. Geochim Cosmochim Acta 44:61–84

Petit AT, Dulong PL (1819) Recherches sur quelques points importants de la theorie de la chaleur. Ann Chim Phys 10:395–413

Raz U (1983) Thermal and volumetric measurements on quartz and other substances at pressures up to 6 kbars and temperatures up to 700° C. Doctoral Thesis, Swiss Fed Inst Tech Zurich 7386

Richet P, Bottinga Y (1982) Modèles de calcul des capacités calorifigues des verres et des liguides silicatés. CR Acad Sci 295, 1121–1124

Richet P, Bottinga Y, Denielou L, Petitet JP, Tequi C (1982) Thermodynamic properties of quartz, cristobalite and amorphous SiO_2: drop calorimetry measurements between 1,000 and 1,800 K and a review from 0 to 2,000 K. Geochim Cosmochim Acta 46:2639–2658

Richet P, Bottinga Y, Tequi C (1984) Heat capacity of sodium silicate liquids. J Am Ceram Soc 88:C6–C8

Robie RA, Bethke PM, Beardsley KM (1967) Selected x-ray crystallographic data, molar volumes, and densities of minerals and related substances. USGS Bull 1248:87p

Robie RA, Finch CB, Hemingway BS (1982a) Heat capacity and entropy of fayalite (Fe_2SiO_4) between 5.1 and 383 K: comparison of calorimetric and equilibrium values for the QFM buffer reaction. Am Mineral 67:463–469

Robie RA, Haselton HT Jr, Hemingway BS (1984) Heat capacities and entropies of rhodochrosite ($MnCO_3$) and siderite ($FeCO_3$) between 5 and 600 K. Am Mineral 69:349–357

Robie RA, Hemingway BS (1984) Entropies of kyanite, andalusite, and sillimanite: additional constraints on the pressure and temperature of the Al_2SiO_5 triple point. Am Mineral 69:298–306

Robie RA, Hemingway BS, Fisher JR (1979) Thermodynamic Properties of Minerals and Related Substances at 298.15 K and 1 Bar (10^5 Pascals) Pressure and at Higher Temperatures. USGS Bull 1452:456p

Robie RA, Hemingway BS, Takei H (1982b) Heat capacities and entropies of Mg_2SiO_4, Mn_2SiO_4, and Co_2SiO_4 between 5 and 380 K. Am Mineral 67:470–482

Robie RA, Hemingway BS, Wilson WH (1976) The heat capacities of calorimetry conference copper and of muscovite $KAl_2(AlSi_3)O_{10}(OH)_2$, pyrophyllite $Al_2Si_4O_{10}(OH)_2$, and illite $K_3(Al_7Mg)(Si_{14}Al_2)O_{40}(OH)_8$ between 15 and 375 K and their standard entropies at 298.15 K. J Res USGS 4:631–644

Robie RA, Hemingway BS, Wilson WH (1978) Low-temperature heat capacities and entropies of feldspar glasses and of anorthite. Am Mineral 63:109–123

Robie RA, Stout JW (1963) Heat capacity from 12 to 305 K and entropy of talc and tremolite. J Phys Chem 67:2252–2256

Robinson GR Jr, Haas JL Jr (1983) Heat capacity, relative enthalpy, and calorimetric entropy of silicate minerals: an empirical method of prediction. Am Mineral 68:541–553

Robinson GR Jr, Haas JL Jr, Schafer CM, Haselton HT Jr (1982) Thermodynamic and thermophysical properties of selected phases in the $MgO-SiO_2-H_2O-CO_2$, $CaO-Al_2O_3-SiO_2-H_2O-CO_2$, $Fe-FeO-Fe_2O_3-SiO_2$ chemical systems, with special emphasis on the properties of basalts and their mineral components. USGS Open-file Rep 83–79:429p

Sharp ZD, Metz GW, Anovitz LM, Essene EJ, Westrum EF Jr, Valley JW (1983) The heat capacity and phase equilibria of monticellite. EOS 64:466

Shomate CH (1946) Heat capacities at low temperatures of the metatitanates of iron, calcium and magnesium. Am Chem Soc J 68:964–966

Shomate CH (1947) Heat capacities at low temperatures of titanium dioxide (rutile and anatase). Am Chem Soc J 69:218–219

Shomate CH, Cook OA (1946) Low-temperature heat capacities and high-temperature heat contents of $Al_2O_3 \cdot 3H_2O$ and $Al_2O_3 \cdot H_2O$. Am Chem Soc J 68:2140–2140

Skinner BJ (1966) Thermal expansion. In: Clark SP (ed) Handbook of Physical Constants, Geol Soc Am Mem 97:75–96

Southard JC (1941) A modified calorimeter for high temperatures. The heat content of silica, wollastonite and thorium dioxide above 25°. Am Chem Soc J 63:3142–3146

Staveley LAK, Linford RG (1969) The heat capacity and entropy of calcite and aragonite, and their interpretation. J Chem Thermodyn 1:1–11

Stebbins JF, Carmichael ISE, Moret LK (1984) Heat capacities and entropies of silicate liquids and glasses. Contrib Mineral Petrol 86:131–148

Stebbins JF, Carmichael ISE, Weill DE (1983) The high temperature liquid and glass heat contents and the heats of fusion of diopside, albite, sanidine and nepheline. Am Mineral 68:717–730

Stout JW, Robie RA (1963) Heat capacity from 11 to 300 K, entropy, and heat of formation of dolomite. J Phys Chem 67:2248–2252

Sumino Y, Anderson OL, Suzuki I (1983) Temperature coefficients of elastic constants of single crystal MgO between 80 and 1,300 K. Phys Chem Min 9:38–47

Thompson AB, Wennemer M (1979) Heat capacities and inversions in tridymite, cristobalite, and tridymite-cristobalite mixed phases. Am Mineral 64:1018–1026

Todd SS (1951) Low-temperature heat capacities and entropies at 298.16 K of crystalline calcium orthosilicate, zinc orthosilicate and tricalcium silicate. Am Chem Soc J 73:3277–3278

Todd SS (1952) Low temperature heat capacities and entropies at 298.16 K of magnesium orthotitanate and magnesium dititanate. Am Chem Soc J 74:4669–4670

Todd SS, Bonnickson KR (1951) Low temperature heat capacities and entropies at 298.16 K of ferrous oxide, manganese oxide and vanadium monoxide. J Am Chem Soc 73:3894–3895

Todd SS, King EG (1953) Heat capacities at low temperatures

and entropies at 298.16 K of titanomagnetite and ferric titanate. Am Chem Soc J 75:4547–4549
Victor AC, Douglas TB (1963) Themodynamic properties of magnesium oxide and beryllium oxide from 298 to 1,200 K. J Res Nat Bur Stand 67A:325–329
Wagner H (1932) Zur Thermochemie der Metasilikate des Calciums und Magnesiums und des Diopsids. Z Anorg Allg Chem 208:1–22
Waldbaum DR (1973) The configurational entropies of $Ca_2MgSi_2O_7-Ca_2SiAl_2O_7$ melilites and related minerals. Contrib Mineral Petrol 39:33–54
Weller WW, Kelley KK (1963) Low-temperature heat capacities and entropies at 298.15 K of akermanite, cordierite, gehlenite, and merwinite. US Bur Mines Rep Inv 6343:7p
Westrum EF Jr, Essene EJ, Perkins D III (1979) Thermophyical properties of the garnet, grossular: $Ca_3Al_2Si_3O_{12}$. J Chem Thermodyn 11:57–66
Westrum EF, Gronvold F (1969) Magnetite (Fe_3O_4). Heat capacity and thermodynamic properties from 5 to 350 K, low-temperature transition. J Chem Thermodyn 1:543–557
White WP (1919) Silicate specific heats. Am J Sci 47:1–21
Winter JK, Ghose S (1979) Thermal expansion and high temperature crystal chemistry of the Al_2SiO_5 polymorphs. Am Mineral 64:573–586

Reveived: March 14, 1984 / Accepted: December 4, 1984